

GA-A27799

HIGH INTERNAL INDUCTANCE FOR STEADY-STATE OPERATION IN ITER AND A REACTOR

by

J.R. FERRON, C.T. HOLCOMB, T.C. LUCE, J.M. PARK, E. KOLEMEN, R.J. LA HAYE,
W.M. SOLOMON, and F. TURCO

AUGUST 2014



DISCLAIMER

This report was prepared as an account of work sponsored by an agency of the United States Government. Neither the United States Government nor any agency thereof, nor any of their employees, makes any warranty, express or implied, or assumes any legal liability or responsibility for the accuracy, completeness, or usefulness of any information, apparatus, product, or process disclosed, or represents that its use would not infringe privately owned rights. Reference herein to any specific commercial product, process, or service by trade name, trademark, manufacturer, or otherwise, does not necessarily constitute or imply its endorsement, recommendation, or favoring by the United States Government or any agency thereof. The views and opinions of authors expressed herein do not necessarily state or reflect those of the United States Government or any agency thereof.

HIGH INTERNAL INDUCTANCE FOR STEADY-STATE OPERATION IN ITER AND A REACTOR

by

J.R. FERRON, C.T. HOLCOMB,* T.C. LUCE, J.M. PARK,† E. KOLEMEN,‡ R.J. LA HAYE,
W.M. SOLOMON,‡ and F. TURCO[¶]

This is a preprint of the synopsis for a paper to be presented at
the Twenty-Fifth IAEA Fusion Energy Conf., October 13-18, 2014
in Saint Petersburg, Russia, and published in the *Proceedings*.

*Lawrence Livermore National Laboratory, Livermore, California.

†Oak Ridge National Laboratory, Oak Ridge, Tennessee.

‡Princeton Plasma Physics Laboratory, Princeton, New Jersey.

¶Columbia University, New York, New York.

Work supported by
the U.S. Department of Energy
under DE-FC02-04ER54698, DE-AC05-00OR22725,
DE-AC02-09CH11466, and DE-FG02-04ER54761

GENERAL ATOMICS PROJECT 30200
AUGUST 2014

High Internal Inductance for Steady-State Operation in ITER and a Reactor

PPC

J.R. Ferron¹, C.T. Holcomb², T.C. Luce¹, J.M. Park³, E. Kolemen⁴, R.J. La Haye¹, W.M. Solomon⁴, and F. Turco⁵

¹General Atomics, P.O. Box 85608, San Diego, CA 92186-5608, USA

²Lawrence Livermore National Laboratory, 7000 East Ave, Livermore, CA 94550, USA

³Oak Ridge National Laboratory, P.O. Box 2008, Oak Ridge, TN 37831, USA.

⁴Princeton Plasma Physics Laboratory, Princeton, New Jersey 08543-0451, USA

⁵Columbia University, 2960 Broadway, New York, NY 10027-6900, USA

ferron@fusion.gat.com

Increased confinement and ideal stability limits at relatively high values of the internal inductance (l_i) have enabled an attractive scenario for steady-state tokamak operation to be demonstrated in DIII-D. The potential of the scenario was shown in double-null divertor discharges with both high elongation and triangularity in which $\beta_N > 4.5$ was achieved at $l_i \approx 1.3$ [Fig. 1(a,b)]. This high value of β_N just reached the ideal $n=1$ kink stability limit calculated without the effect of a stabilizing vacuum vessel wall, with the ideal-wall limit still higher at $\beta_N > 5.5$. Confinement is well above the H-mode level with $H_{98} \approx 1.8$. This type of discharge is a candidate for a reactor that could either operate stably at $\beta_N \approx 4$ without the requirement for a nearby conducting wall or $n \geq 1$ active stabilization coils, or at $\beta_N \approx 5$ with wall stabilization.

For ITER, operation at $l_i \approx 1$ is a promising option for the steady-state mission. Improved core confinement at high l_i could compensate for reduced H-mode pedestal confinement if a low pedestal height results from pedestal physics and/or ELM-stabilization using 3D fields. At $l_i \approx 1$, the self-driven bootstrap current fraction would be $f_{BS} \approx 0.5$ with the remainder from external current drive that is efficient because the current is driven near the axis. This scenario has been tested in the scaled ITER shape in DIII-D at $\beta_N \approx 3.4$ with performance appropriate for the ITER $Q=5$ mission, $\beta_N H_{89}/q_{95}^2 > 0.3$ [Fig. 1(c,e)]. High l_i discharges thus far take advantage of inductively driven current density near the axis as a partial substitute for externally-driven current. Modeling with self-consistent heating, current drive and transport of a potential stationary, fully noninductive double-null divertor discharge in DIII-D finds a solution calculated stable without a conducting wall at $\beta_N=4$, $l_i=1.07$, and $f_{BS}=0.5$ with electron cyclotron current drive (ECCD) and neutral beam current drive near the axis (Fig. 2). A similar solution at $\beta_N=5$ is calculated to be stable with the vacuum vessel wall.

Operation in steady-state requires a compromise between high l_i and high f_{BS} . Increased β_N and strong discharge shaping to raise the β_N limit increase the bootstrap current density in the outer half of the plasma, including in the H-mode pedestal region. Thus l_i will decrease as f_{BS} increases. The discharges in the scaled ITER shape aimed at a compromise set of parameters expected to be self-consistent for steady-state operation [1] with $l_i \approx 1$, $\beta_N \approx 4$, $f_{BS} \approx 0.5$. The experiment thus far has reached somewhat lower β_N at $q_{95}=4.8$, yielding $f_{BS} \approx 0.4$

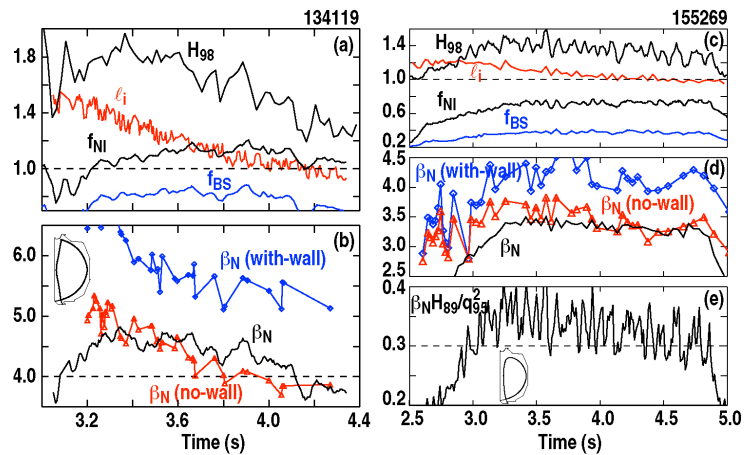


Fig. 1. Parameters in high l_i discharges in (a,b) a double-null divertor shape, (c-e) the ITER shape scaled to fit the DIII-D vacuum vessel. β_N (with-wall) and β_N (no-wall) are the calculated $n=1$ ideal MHD stability limits with and without the DIII-D vacuum vessel, respectively.

and noninductive current fraction $f_{NI} \approx 0.7$ [Fig. 1(c)]. In contrast, with high β_N and relatively high $q_{95} = 7$, the double null divertor discharge is overdriven with $f_{BS} \approx 0.8$, $f_{NI} > 1$ and negative surface voltage [Fig. 1(a)]. The noninductive current overdrive was confirmed through an increase in the total plasma current when the inductive coil current was held constant.

Reduced H-mode pedestal height self-consistently results in increased l_i through the reduction in pedestal bootstrap current density. Thus a high l_i scenario is compatible with variants of H-mode in which ELMs are absent and the pedestal pressure and current density are somewhat reduced (e.g. I-mode, 3D field ELM stabilization). This self-consistency was explored in DIII-D through the use of $n=3$ fields to modify the pedestal. Increased l_i was observed as the $n=3$ field amplitude was increased and the pedestal pressure decreased. Optimization to the minimum possible $q(0)$ also increased l_i leading to $q(0) \approx 1$ but without observation of sawteeth.

Global, ideal, low toroidal mode number pressure and current driven instabilities, which are expected to set the ultimate limit to pressure in these discharges, have not yet been observed. The limit to performance is normally an $m=2/n=1$ resistive tearing mode which is often triggered by an $m=1/n=1$ fishbone instability-like burst. At $q_{95} = 4.5$ to 6, the resistive $n=1$ mode limited the maximum β_N to 3.8–4 in both discharge shapes even though the calculated, ideal $n=1$ β_N limits in the scaled ITER shape are below those in the double-null shape (Fig. 1). However, at $q_{95} = 7$ in the double null shape, β_N was limited to just below 5, not by instability, but rather by available heating power.

Modeling projects that parameters for stationary, high l_i , fully noninductive operation are attainable in DIII-D. Studies with model equilibria documented the scaling of l_i with the pedestal current density [Fig. 2(a)]. An increase of l_i from 0.75 to 1.3 requires a factor of two decrease in the pedestal current, with $l_i \approx 1$ at about 75% of the reference experimental value. There is a corresponding increase in the $n=1$ no-wall β_N limit, which reaches $\beta_N \approx 5$ with $l_i \approx 1.3$, similar to what was observed in the double-null experimental discharges. Thus there is

a significant advantage in stability if current density is shifted from the pedestal region to the core. In order to maintain $q(0) > 1$ to avoid sawteeth, the width of the current density peak near the axis must increase as q_{95} is reduced, so that some of the externally-driven current must be located off-axis. Studies with the FASTRAN transport code using the TGLF energy transport model explored how the increased current drive power in a proposed DIII-D upgrade (13

MW off-axis neutral beam, 9 MW ECCD) could be applied to maintain a stationary, $f_{NI} = 1$ high l_i discharge. In the solution, the bootstrap current density profile is broad [Fig. 2(b)] and off-axis neutral beam current drive coupled with ECCD close to the axis is used to generate the current density peak extending to about $\rho \approx 0.4$ that maintains the increased value of l_i .

Thus, modeling and experiment are showing the potential of a high l_i discharge for fully noninductive, stationary operation. Keys to full development of this scenario are an understanding of how to maximize l_i through access to appropriate pedestal parameters, avoidance of the performance limiting $n=1$ tearing mode, and demonstration of the total required externally-driven current near the axis.

This work was supported by the US Department of Energy under DE-FC02-04ER54698, DE-AC52-07NA27344, DE-AC05-00OR22725, DE-AC02-09CH11466, and DE-FG02-04E54761.

[1] Y.R. Lin-Liu, et al., Phys. Plasmas **6**, 3934 (1999).

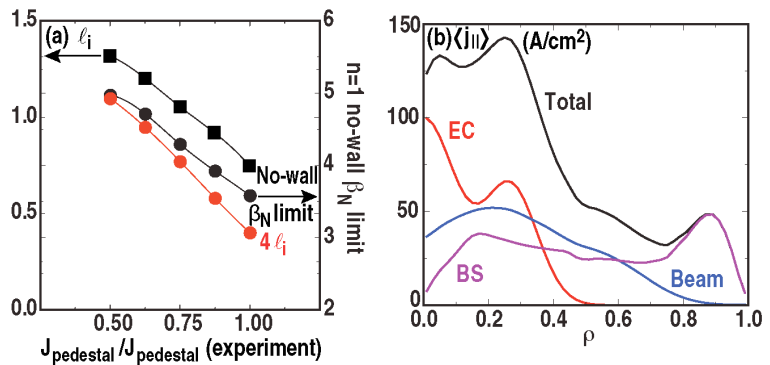


Fig. 2. (a) Scaling in model equilibria of l_i (squares) and the calculated $n=1$ no-wall β_N limit (circles) with the H-mode pedestal current density, and (b) current density profiles in the $\beta_N=4$ transport code-modeled steady-state solution for DIII-D.